ISSN 1070-3284, Russian Journal of Coordination Chemistry, 2013, Vol. 39, No. 12, pp. 849–856. © Pleiades Publishing, Ltd., 2013.
Original Russian Text © L.D. Popov, S.I. Levchenkov, I.N. Shcherbakov, V.V. Minin, G.G. Aleksandrov, E.A. Ugolkova, V.V. Lukov, V.A. Kogan, 2013, published in Koordinatsionnaya Khimiya, 2013, Vol. 39, No. 12, pp. 743–750.

Polymeric Copper(II) Complexes with 4-Formyl-3-Methyl-1-Phenylpyrazol-5-one Hetarylhydrazones: Synthesis and Crystal Structures

L. D. Popov[a], S. I. Levchenkov[b, *], I. N. Shcherbakov[a], V. V. Minin[c], G. G. Aleksandrov[c], E. A. Ugolkova[c], V. V. Lukov[a], and V. A. Kogan[a]

[a] *Southern Federal University, Rostov-on-Don, Russia*

[b] *Southern Scientific Center, Russian Academy of Sciences, Rostov-on-Don, Russia*

[c] *Kurnakov Institute of General and Inorganic Chemistry, Russian Academy of Sciences, Leninskii pr. 31, Moscow, 119991 Russia*

**e-mail: s.levchenkov@gmail.com*

Received March 20, 2013

Abstract—4-Formyl-3-methyl-1-phenylpyrazol-5-one quinolin-2-yl- (H_2L^1) and benzothiazol-2-ylhydrazones (H_2L^2) were synthesized and studied. Quantum-chemical modeling of possible tautomers of the hydrazones was performed. Copper(II) complexes of the general formula [Cu(HL)(ROH)]Y (R = CH_3, C_2H_5; Y = NO_3, ClO_4) were obtained and examined by IR and EPR spectroscopy, magnetochemistry, and X-ray diffraction. Additional coordination through the N atom of the pyrazole ring enables the complex molecules to form zigzag polymer chains linked by intermolecular hydrogen bonds.

DOI: 10.1134/S1070328413110079

INTRODUCTION

Development of the coordination chemistry of acylpyrazolones and their derivatives is due to their high ligating ability and biological activity [1–5]. From the theoretical viewpoint, compounds of this class are also interesting because of their plentiful tautomerism [1, 2, 6, 7]. Although complexes of acylhydrazones and thiosemicarbazones of 4-formylpyrazolones have been extensively examined [6, 8–12], the ligating ability of 4-formylpyrazolone hetarylhydrazones remains poorly studied.

We obtained new ligand systems, namely, 4-formyl-3-methyl-1-phenylpyrazol-5-one quinolin-2-ylhydrazone (H_2L^1) and 4-formyl-3-methyl-1-phenylpyrazol-5-one benzothiazol-2-ylhydrazone (H_2L^2), and their copper(II) complexes $[Cu(HL^1)(EtOH)]NO_3$ (**I**), $[Cu(HL^1)(EtOH)]ClO_4$ (**II**), $[Cu(HL^2)(MeOH)]NO_3$ (**III**), and $[Cu(HL^2)(MeOH)]ClO_4$ (**IV**).

EXPERIMENTAL

Synthesis of hydrazones H_2L^1 and H_2L^2. A hot solution of 2-hydrazinoquinoline or 2-hydrazinobenzothiazole (5 mmol) in ethanol (10 mL) was added to a hot solution of 4-formyl-3-methyl-1-phenylpyrazol-5-one (5 mmol) in ethanol (10 mL). The reaction mixture was refluxed for 4 h and left overnight. The precipitate that formed was filtered off and recrystallized from butanol–DMF (4 : 1).

The yield of H_2L^1 was 1.17 g (68%), T_m = 176°C.

For $C_{20}H_{17}N_5O$			
anal. calcd., %:	C, 69.96;	H, 4.99;	N, 20.39.
Found, %:	C, 70.11;	H, 4.84;	N, 20.52.

^{1}H NMR (DMSO-d_6), δ (ppm): 2.18 s (3H, Me), 6.99 d (1H, H(3), quinoline, J = 9.4 Hz), 7.10 t (1H, *p*-Ph, J = 7.3 Hz), 7.203 s (1H, CH, azomethine), 7.34–7.40 m (3H, *m*-Ph, H(8), quinoline), 7.66 t (1H, H(7), quinoline, J = 7.7 Hz), 7.81–7.86 m (2H, H(5), H(6), quinoline), 7.99 d (2H, *o*-Ph, J = 7.8 Hz), 8.15 d (1H, H(4), quinoline, J = 9.4 Hz), 12.83 s (1H, NH), 17.67 s (1H, NH).

IR (ν, cm^{-1}): 3390, 3188 ν(NH), 1640 ν(C=O), 1589 ν(C=N).

The yield of H_2L^2 was 0.96 g (55%), T_m = 198°C.

For $C_{18}H_{15}N_5OS$			
anal. calcd., %:	C, 61.88;	H, 4.33;	N, 20.04.
Found, %:	C, 62.05;	H, 4.46;	N, 19.90.

^{1}H NMR (DMSO-d_6), δ (ppm): 2.49 s (3H, Me), 7.09 t (1H, *p*-Ph, J = 7.8 Hz), 7.28–7.40 m (2H, CH_{arom}, J = 8.1 Hz), 7.50–7.65 m (5H, CH_{arom}), 7.77 d (1H, CH_{arom}, J = 7.5 Hz), 8.084 s (1H, CH_{azomet}), 12.20 s (1H, NH), 17.09 s (1H, NH).

IR (ν, cm^{-1}): 3408, 3185 ν(NH), 1632 ν(C=O), 1580 ν(C=N).

Synthesis of complexes I and II. A solution of copper(II) nitrate or copper(II) perchlorate (1 mmol) in methanol (10 mL) was added to a hot solution of the hydrazone H_2L^1 (1 mmol) in ethanol (20 mL). The reaction mixture was refluxed for 1 h. After cooling, the precipitate that formed was filtered off and recrystallized from ethanol.

The yield of complex **I** was 0.23 g (45%), T_m > 250°C, μ_{eff} = 1.89 (300 K) and 1.88 μ_B (77.4 K).

For $C_{22}H_{22}CuN_6O_5$

anal. calcd., %:	C, 51.4;	H, 4.31;	N, 16.4;	Cu, 12.4.
Found, %:	C, 51.7;	H, 4.22;	N, 16.0;	Cu, 12.6.

IR (ν, cm^{-1}): 3377 ν(OH), 3193 ν(NH), 1625, 1595 ν(C=N).

The yield of complex **II** was 0.19 g (35%), T_m > 250°C, μ_{eff} = 1.85 (300 K) and 1.83 μ_B (77.4 K).

For $C_{22}H_{22}CuN_5O_6Cl$

anal. calcd., %:	C, 47.9;	H, 4.02;	N, 12.7;	Cu, 11.5.
Found, %:	C, 48.3;	H, 4.00;	N, 12.9;	Cu, 11.7.

IR (ν, cm^{-1}): 3461 ν(OH), 3191 ν(NH), 1621, 1595 ν(C=N).

Synthesis of complexes III and IV. A solution of copper(II) nitrate or copper(II) perchlorate (1 mmol) in methanol (10 mL) was added to a suspension of the hydrazone H_2L^2 (1 mmol) in hot methanol (20 mL). The hydrazone dissolved immediately. The reaction mixture was refluxed for 3 h. After cooling, the precipitate that formed was filtered off and washed with methanol.

The yield of complex **III** was 0.18 g (35%), T_m > 250°C. μ_{eff} 1.90 (300 K) and 1.91 μ_B (77.4 K).

For $C_{19}H_{18}CuN_6O_5S$

anal. calcd., %:	C, 45.1;	H, 3.59;	N, 16.6;	Cu, 12.6.
Found, %:	C, 44.8;	H, 3.67;	N, 17.0;	Cu, 12.3.

IR (ν, cm^{-1}): 3460 ν(OH), 3220 ν(NH), 1620, 1595 ν(C=N).

The yield of complex **IV** was 0.16 g (30%), T_m > 250°C, μ_{eff} = 1.87 (300 K) and 1.87 μ_B (77.4 K).

For $C_{19}H_{18}ClCuN_5SO_6$

anal. calcd., %:	C, 42.0;	H, 3.34;	N, 12.9;	Cu, 11.7.
Found, %:	C, 42.6;	H, 3.45;	N, 12.4;	Cu, 11.5.

IR (ν, cm^{-1}): 3479 ν(OH), 3230 ν(NH), 1617, 1597 ν(C=N).

^{1}H NMR spectra were recorded on a Varian Unity 300 spectrometer (300 MHz) in the pulse Fourier transform mode in DMSO-d_6 with HMDS as the internal standard.

IR spectra (Nujol) were recorded on a Varian Scimitar 1000 FTIR instrument in the 400–4000 cm^{-1} range.

Specific magnetic susceptibility was measured using the relative Faraday method in a temperature range from 77.4 to 300 K.

X-ray diffraction study of complexes I and IV was performed on a Bruker Apex II diffractometer (MoK_α, radiation, λ = 0.71073 Å, graphite monochromator). The collected set of reflection intensities was processed with the SAINT [13] and SADABS programs [14]. The structures were solved by the direct methods and refined anisotropically on F^2_{hkl} by the full-matrix least-squares method for non-hydrogen atoms. Hydrogen atoms were located geometrically and refined using a riding model (U_{iso}(H) = nU_{iso}(C), where n = 1.5 for the methyl C atoms and n = 1.2 for the other C atoms). All calculations were performed with the SHELX program package [15]. The molecular geometry of the complexes was analyzed using the PLATON program [16].

Crystallographic parameters and the data collection and refinement statistics for structures **I** and **IV** are summarized in Table 1. Selected bond lengths and bond angles are given in Table 2; hydrogen bond parameters are given in Table 3. The atomic coordinates and thermal parameters have been deposited with the Cambridge Crystallographic Data Centre (nos. 909689 (**I**) and 909690 (**IV**); deposit@ccdc.cam.ac.uk or http://www.ccdc.cam.ac.uk).

Quantum-chemical DFT computations were performed using the hybrid exchange-correlation functional B3LYP [17–19] and the extended split-valence basis set 6-311G+(*d*,*p*) with the Gaussian'03 program [20]. The results of the calculations were visualized and graphically represented with the Chemcraft program [21].

EPR spectra were recorded on a Bruker E-680X ELEXSYS radio spectrometer in the X range at room temperature. The stable diphenylpicrylhydrazyl radical was used as a standard. The parameters of the spin Hamiltonian were determined by minimizing an error functional for the best fit of a theoretical spectrum to the experimental one:

$$F = \frac{1}{N}\sum_{i=1}^{N}\left(Y_i^T - Y_i^E\right)^2, \quad (1)$$

where Y_i^E is the array of experimental EPR signal intensities for a constant magnetic field strength (H) increment, Y_i^T are the theoretical EPR signal intensities calculated at the same field strengths H, and N is the number of points.

Theoretical EPR spectra were modeled as described in [22]. A sum of the Lorentzian and Gaussian functions was used as a function for line shapes

[23]. According to relaxation theory [24], the line widths were given by the formula

$$\Delta H = \alpha + \beta m_I + \gamma m_I^2, \quad (2)$$

where m_I is the projection of the nuclear spin onto the magnetic field vector and α, β, and γ are parameters. In the minimization procedure, *g* factors, hyperfine constants, and line widths and shapes were varied.

RESULTS AND DISCUSSION

Compounds H_2L^1 and H_2L^2 as well as other 4-formyl-3-methyl-1-phenylpyrazol-5-one hydrazones can exist as a number of tautomers. These can be divided into two groups: pyrazolone and hydroxypyrazole tautomers, the former being more stable in the majority of cases [6, 25].

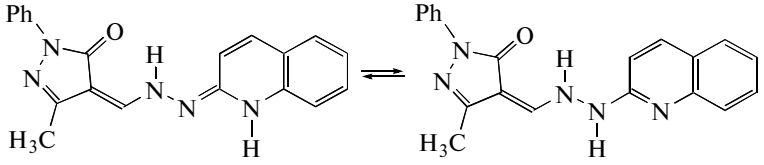

(H_2L^1a) (H_2L^1b)

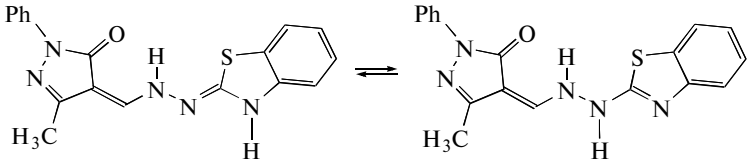

(H_2L^2a) (H_2L^2b)

To determine the most stable species for the hydrazones H_2L^1 and H_2L^2, we effected quantum-chemical calculations of the geometry and total energies of all possible tautomers in vacuo and in solutions ($CHCl_3$ and DMSO). The pyrazolone tautomers H_2L^1a (quinolone) and H_2L^2a (benzothiazolone) proved to be always most stable. The second pyrazolone tautomer H_2L^1b is less stable than H_2L^1a in vacuo and in $CHCl_3$ and DMSO by 0.95, 0.62, and 0.05 kcal/mol, respectively. For H_2L^2, the energy difference between these tautomers is much larger: 3.00, 2.56, and 1.89 kcal/mol, respectively.

According to the calculated energies, both pyrazolone tautomers H_2L^1a and H_2L^1b could coexist in DMSO. However, ^1H NMR spectra provide evidence that the quinolone-pyrazolone species H_2L^1a is the main tautomer in this case as well, because the coupling constant for the H(3) and H(4) protons of the quinoline moiety is 9.5 Hz. For the quinoline tautomer H_2L^1b, this constant would be ~8 Hz.

The lowest-energy hydroxypyrazole tautomers of the hydrazones H_2L^1 and H_2L^2 are less stable in vacuo than H_2L^1a and H_2L^2a by 2.59 and 3.88 kcal/mol, respectively. In $CHCl_3$ and DMSO, the energy difference increases substantially: 5.89 and 6.64 kcal/mol for H_2L^1 and 7.25 and 8.28 kcal/mol for H_2L^2.

Reactions of the hydrazones H_2L^1 and H_2L^2 with copper(II) nitrate and copper(II) perchlorate afforded the complexes $[Cu(HL^1)(ROH)]NO_3$ and $[Cu(HL^2)(ROH)]ClO_4$, respectively (R = C_2H_5 (**I, II**) and CH_3 (**III**, **IV**)). Complexes **I** and **IV** were structurally characterized by X-ray diffraction.

The organic ligand in complex **I** is monodeprotonated and coordinated in a tridentate fashion. The coordination polyhedron of the copper atom is a distorted trigonal bipyramid (Fig. 1). The equatorial plane is made up of the O(2) atom of the coordinated ethanol molecule, the azomethine N(3) atom, and the N(4*B*) atom of the pyrazole ring of an adjacent complex molecule. The apical positions are occupied by the O(1) atom and the quinoline N(1) atom. The Cu atom deviates from the equatorial plane by only 0.009 Å toward the O(1) atom. The six-membered chelate ring is virtually planar; the largest deviation from the mean-square plane is 0.040 Å (C(12)). The five-membered chelate ring adopts an envelope conformation, with the copper atom deviating from the mean-square plane of the other four atoms by 0.141 Å. Both chelate rings are virtually coplanar with the quinoline moiety. The monodeprotonated tridentate organic ligand is nearly planar; the dihedral angle between the mean-square planes of the pyrazole and quinoline rings is 10.25°. The planes of the phenyl and pyrazole rings make an angle of 55.04°.

Because the coordination polyhedron of the Cu atom comprises the N atom of an adjacent molecule, the mononuclear species form infinite zigzag polymer chains along the crystallographic axis *y* in the crystal (Fig. 2). The dihedral angle between the planes of the electron-donating atoms O(1)N(3)N(1) in the neighboring mononuclear species is 64.71°. In the crystal of complex **I**, polymer chains are linked by hydrogen bonds involving the O(3) atom of the outer-sphere nitrate ion and the H(2*C*) and H(2*B*) atoms of two mononuclear fragments (Table 3).

Table 1. Crystallographic parameters and the data collection and refinement statistics for structures **I** and **IV**

Parameter	Value	
	I	**IV**
M	514.00	543.43
Crystal dimensions, mm	0.15 × 0.09 × 0.05	0.28 × 0.12 × 0.07
Crystal system	Monoclinic	Monoclinic
Space group	$P2_1/n$	$P2_1/n$
a, Å	11.635(2)	11.1808(15)
b, Å	12.176(3)	12.5889(18)
c, Å	15.065(3)	15.123(2)
β, deg	95.917(6)	99.409(3)
V, Å^3	2122.8(8)	2100.0(5)
Z	4	4
ρ_{calcd}, g/cm^3	1.608	1.719
μ, mm^{-1}	1.08	1.317
F(000)	1060	1108
$2\theta_{max}$, deg	50.8	59.6
Ranges of h, k, and l indices	$-12 < h < 14$, $-14 < k < 14$, $-18 < l < 18$	$-15 < h < 12$, $-17 < k < 17$, $-21 < l < 12$
Number of measured reflections	15584	14320
Number of unique reflections	3891	5901
Number of reflections with $I \geq 2\sigma(I)$	1854	3558
Number of parameters refined	302	302
GOOF (for all reflections)	0.999	1.000
R_1 ($I > 2\sigma(I)$)	0.0739	0.0614
wR_2 (for all reflections)	0.1785	0.1609
$\Delta\rho_{max}/\Delta\rho_{min}$, e Å^{-3}	1.233/–0.997	1.509/–0.836

Structure **IV** (Fig. 3) is similar to structure **I** and has close crystallographic parameters. The residue of 4-formyl-3-methyl-1-phenylpyrazol-5-one benzothiazol-2-ylhydrazone is monodeprotonated and coordinated in a tridentate fashion. The coordination polyhedron of the copper atom is a distorted trigonal bipyramid. The equatorial plane is made up of the O(2) atom of the coordinated methanol molecule, the azomethine N(3) atom, and the N(5*B*) atom of the pyrazole ring of an adjacent complex molecule. The apical positions are occupied by the O(1) atom and the N(1) atom of the benzothiazole ring.

As in complex **I**, additional coordination of the Cu atom to the N atom of the pyrazole ring of an adjacent molecule in complex **IV** enables its mononuclear species to form infinite zigzag polymer chains along the

Table 2. Selected bond lengths and bond angles in the coordination polyhedra of the copper atoms in structures **I** and **IV***

Bond	*d*, Å	Bond	*d*, Å
	I		
Cu(1)–N(3)	1.980(6)	Cu(1)–O(1)	1.929(5)
Cu(1)–N(1)	1.985(6)	Cu(1)–O(2)	2.121(6)
Cu(1)–N(4)^{i}	2.102(6)	O(1)–C(12)	1.277(9)
	IV		
Cu(1)–N(1)	1.973(3)	Cu(1)–O(1)	1.931(3)
Cu(1)–N(3)	2.013(3)	Cu(1)–O(2)	2.225(3)
Cu(1)–N(5)^{i}	2.094(3)	O(1)–C(10)	1.278(5)
Angle	ω, deg	Angle	ω, deg
	I		
O(1)Cu(1)N(3)	92.5(2)	N(1)Cu(1)N(4)^{i}	96.9(2)
O(1)Cu(1)N(1)	171.7(2)	O(1)Cu(1)O(2)	86.2(2)
N(3)Cu(1)N(1)	81.0(3)	N(3)Cu(1)O(2)	128.5(2)
O(1)Cu(1)N(4)^{i}	91.3(2)	N(1)Cu(1)O(2)	93.8(2)
N(3)Cu(1)N(4)^{i}	131.3(3)	N(4)^{i}Cu(1)O(2)	100.2(2)
	IV		
O(1)Cu(1)N(1)	167.95(13)	N(3)Cu(1)N(5)^{i}	135.70(13)
O(1)Cu(1)N(3)	92.10(12)	O(1)Cu(1)O(2)	86.38(12)
N(1)Cu(1)N(3)	79.99(13)	N(1)Cu(1)O(2)	91.11(13)
O(1)Cu(1)N(5)^{i}	95.49(12)	N(3)Cu(1)O(2)	126.91(13)
N(1)Cu(1)N(5)^{i}	96.52(13)	N(5)^{i}Cu(1)O(2)	97.14(13)

* The symmetry operation codes are ^{i} $-x + 1/2, y + 1/2, -z + 1/2$ for **I** and ^{i} $-x + 1/2, y + 1/2, -z + 1/2$ for **IV**.

Table 3. Parameters of the intermolecular hydrogen bonds in the crystals of complexes **I** and **IV***

Hydrogen bond D–H···A	Distance, Å			Angle DHA, deg
	D–H	H···A	D···A	
	I			
O(2)–H(2C)···O(3S)	0.95	2.46	2.702(9)	94
N(2)–H(2*B*)···O(3S)^{i}	0.88	1.90	2.757(9)	165
	IV			
N(2)–H(2*A*)···O(4S)	0.88	2.18	2.951(5)	146
N(2)–H(2*A*)···O(3S)	0.88	2.26	3.048(5)	149
O(2)–H(2)···O(4S)^{ii}	0.86	2.29	2.867(6)	125

* The coordinates of the primed atoms: ^{i} $1 - x, -y, -z$; ^{ii} $1 - x, 1 - y, -z$.

crystallographic axis *y* (Fig. 4). The chains are united into a 3D framework through the hydrogen bonds N(2)–H(2*A*)···O(4S), N(2)–H(2*A*)···O(3S), and O(2)–H(2)···O(4S) (Table 3). The dihedral angle between the planes of the electron-donating atoms O(1)N(3)N(1) in the neighboring mononuclear species of complex **IV**

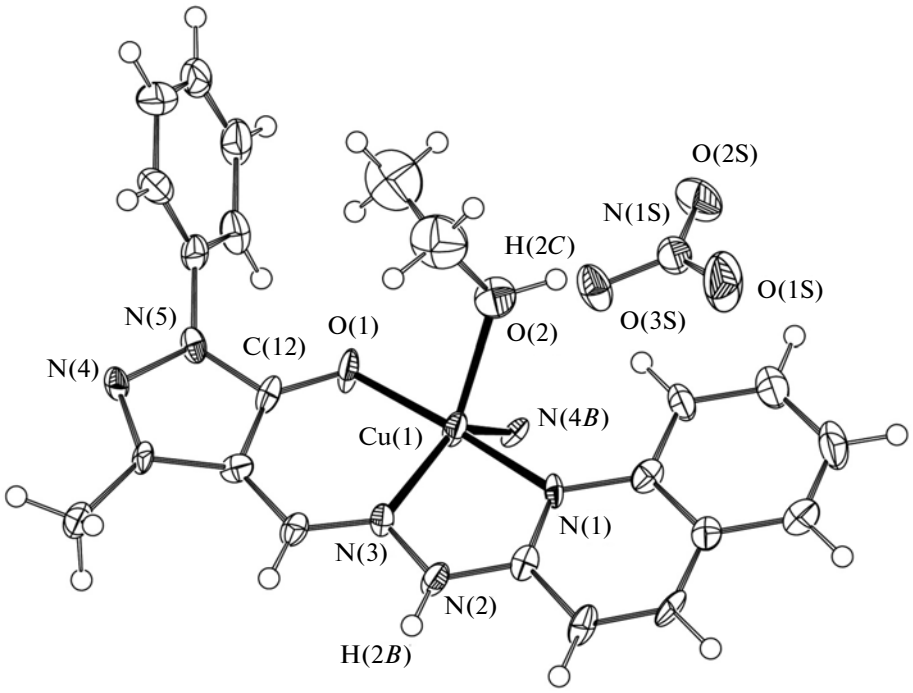

Fig. 1. Structure **I** with atomic thermal displacement ellipsoids (50% probability).

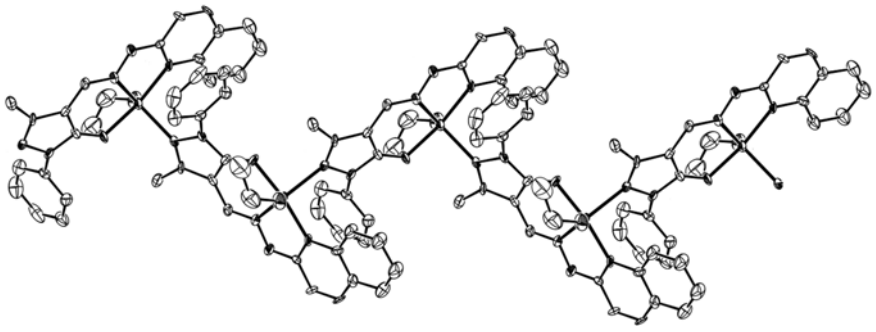

Fig. 2. Polymer chains in the crystal of complex **I** (the nitrate ions and the hydrogen atoms are omitted).

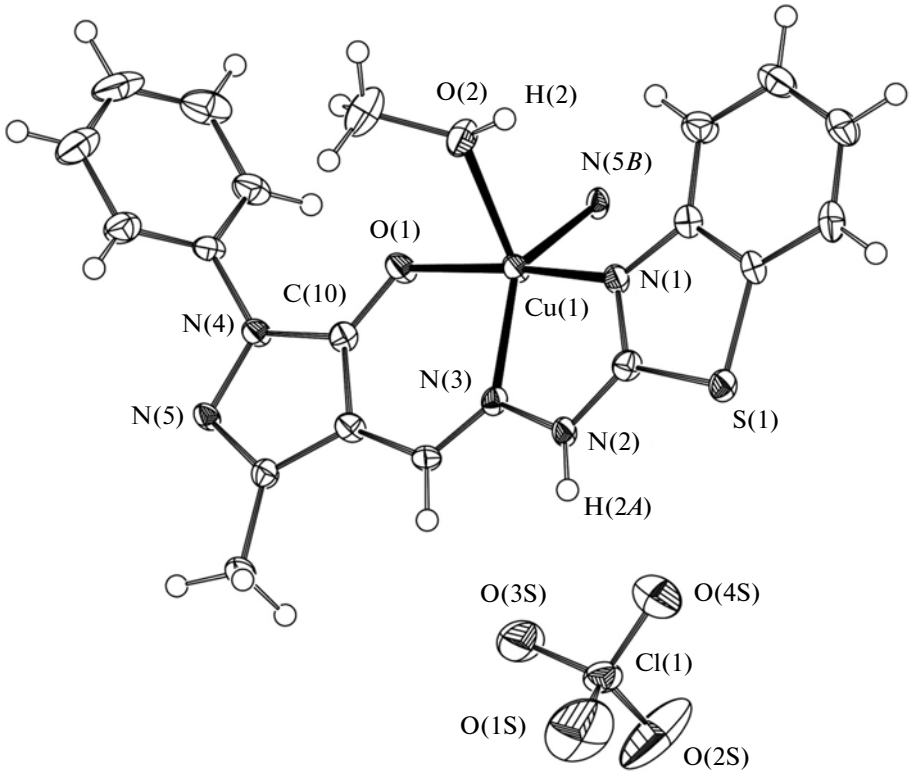

Fig. 3. Structure **IV** with atomic thermal displacement ellipsoids (50% probability).

is somewhat smaller than that in complex **I** (59.34°). Nevertheless, the copper–copper distances in the polymer chains of complexes **I** and **IV** are nearly the same: 7.058 and 7.091 Å, respectively.

The EPR spectra (Fig. 5) of polycrystalline samples of complexes **I** and **IV** show ill-resolved lines in the parallel and perpendicular orientations of the *g* tensor with the following spin Hamiltonian parameters: $g_{\|} = 2.2215$ and $g_{\perp} = 2.0862$ for complex **I** and $g_{\|} = 2.2520$ and $g_{\perp} = 2.0875$ for complex **IV**. These spin Hamiltonian parameters correspond to square planar Cu(II) complexes with oxygen and nitrogen in the first coordination sphere. The wider EPR lines for complex **IV** compared to those for complex **I** are due to the bulkier equatorial substituent (EtOH) in **I** and the smaller one (MeOH) in **IV**, which produces a less "rigid" environment of the metal ion in the polymer matrix.

The absence of a half-field signal for a forbidden transition characteristic of exchange-coupled systems with the electron spin $S = 1$ suggests the absence of exchange effects in complexes **I** and **IV**, though magnetic exchange through a rather long chain of σ-bonds has been repeatedly noted earlier for copper complexes [26, 27]. The conclusion about the absence of magnetic exchange is confirmed by magnetochemical data: the effective magnetic moments of complexes **I**–

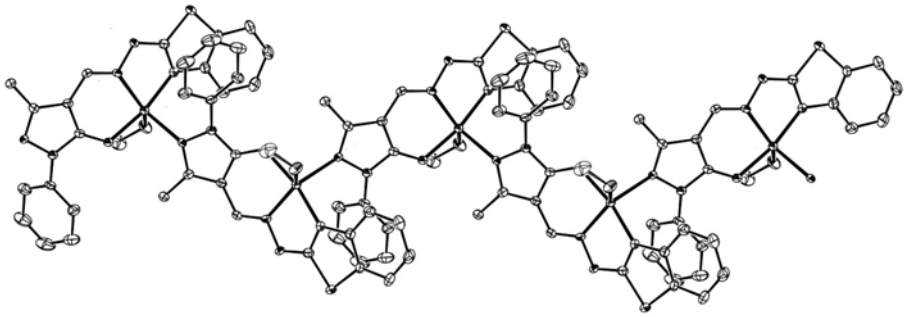

Fig. 4. Polymer chains in the crystal of complex **IV** (the perchlorate ions and the hydrogen atoms are omitted).

IV at room temperature are somewhat higher than the pure spin value and remain virtually unchanged on cooling to 77.4 K.

When dissolved in DMF, the complexes under study decompose; in less polar dichloromethane, they form suspensions, probably by degradation of the polymer chain into mononuclear species. The EPR spectrum of a suspension of complex **I** (Fig. 6) differs noticeably from the spectrum of its polycrystalline sample. It can be described by a distorted (in a rhombic way) spin Hamiltonian with the hyperfine coupling

$$\begin{aligned}\hat{H}_{\text{solid}} &= g_z\beta H_z\hat{S}_z + g_x\beta H_x\hat{S}_x + g_y\beta H_y\hat{S}_y \\ &+ A\hat{I}_z\hat{S}_z + B\hat{I}_x\hat{S}_x + C\hat{I}_y\hat{S}_y,\end{aligned} \quad (3)$$

where g_z, g_x, and g_y are the z, x, y components of the g tensor, A, B, and C are the components of the hyperfine structure tensor, the S_z, S_x, and S_y are the projections of the spin operator of the monomer onto the coordinate axes, $S = 1/2$, I_z, I_x, and I_y are the projections of the nuclear spin operator of the central atom of the monomer onto the coordinate axes, $I = 3/2$.

The spin Hamiltonian parameters of the EPR spectrum of a suspension of complex **I** in CH_2Cl_2 are as follows: $g_z = 2.074$, $A = 4.91 \times 10^{-3}$ cm^{-1}, $g_x = 2.145$, $B = 9.93 \times 10^{-3}$ cm^{-1}, $g_y = 2.183$, $C = 4.92 \times 10^{-3}$ cm^{-1}.

The EPR spectrum obtained differs in spin Hamiltonian parameters from the axially symmetrical spectrum of Cu(II) with the $d_{x^2-y^2}$, ground state of the central atom, for which $g_{||} > g_\perp$ and $A > B$. It rather corresponds to the fairly uncommon d_{z^2}, ground state of copper, for which $g_\perp > g_{||}$ and $B < A$. The ground state of Cu(II) changes when its square planar chelate ring undergoes tetrahedral or other distortions. The type of distortions occurring in this case cannot be specified because we are unaware of the composition and structure of a fragment formed by degradation of the polymer chain.

To sum up, we obtained and studied 4-formyl-3-methyl-1-phenylpyrazol-5-one hetarylhydrazones as new ligand systems and performed quantum-chemical modeling of their tautomeric species. A series of new copper(II) complexes with these ligands were synthe-

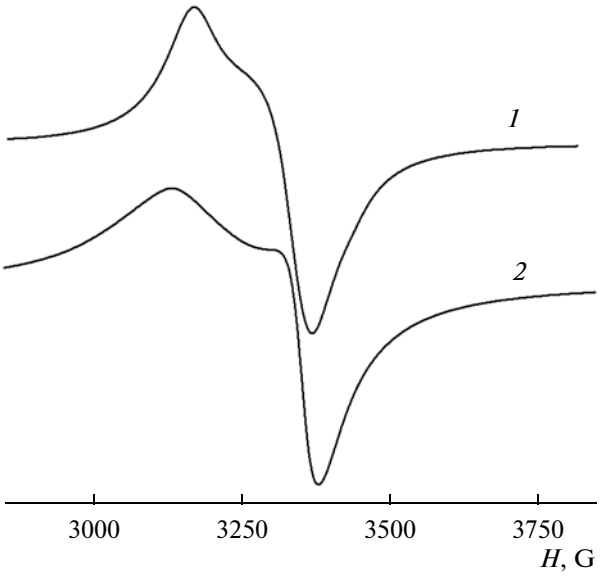

Fig. 5. EPR spectra of polycrystalline samples of complexes **I** (*1*) and **IV** (*2*) at 293 K.

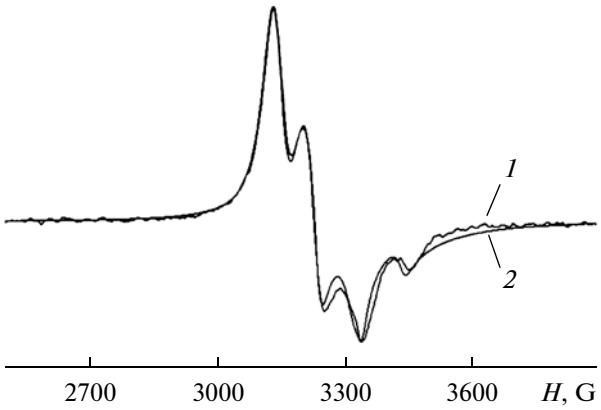

Fig. 6. (*1*) Experimental and (*2*) theoretical EPR spectra of a suspension of complex **I** in CH_2Cl_2 at 293 K.

sized, structurally characterized, and examined by physicochemical methods. Because of additional coordination through the N atom of the pyrazole ring, these complexes form zigzag polymer chains.

REFERENCES

1. Garnovskii, A.D., Nivorozhkin, A.L., and Minkin, V.A., *Coord. Chem. Rev.*, 1993, vol. 126, nos. 1–2, p. 1.
2. Marchetti, F., Pettinari, C., and Pettinari, R., *Coord. Chem. Rev.*, 2005, vol. 249, no. 24, p. 2909.
3. Casas, J.S., Garsia-Tasende, M.S., Sanchez, A., et al., *Coord. Chem. Rev.*, 2007, vol. 251, nos. 11–12, p. 1561.
4. Kurdekar, G.S., Sathisha, M.P., Budagumpi, S., et al., *Med. Chem. Res.,* 2012, vol. 21, no. 9, p. 2273.
5. Garnovskii, A.D. and Vasil'chenko, I.S., *Usp. Khim.*, 2005, vol. 74, no. 3, p. 211.
6. Minkin, V.I., Garnovskii, A.D., Elguero, J., et al., *Adv. Heterocycl. Chem.*, 2000, vol. 76, p. 157.
7. Movchan, A.I., Kurbangalieva, A.R., Kataeva, O.N., et al., *Russ. J. Gen. Chem.*, 2003, vol. 73, no. 7, p. 1130.
8. Zhang, L., Liu, L., Jia, D., et al., *Inorg. Chem. Commun.*, 2004, vol. 7, no. 12, p. 1306.
9. Lu, J., Zhang, L., Liu, L., et al., *Spectrochim. Acta, Part A*, 2008, vol. 71, no. 3, p. 10361.
10. Shul'gin, V.F., Obukh, A.I., Rusanov, E.B., et al., *Russ. J. Inorg. Chem.*, 2009, vol. 54, no. 8, p. 1223.
11. Modi, C.K., Jani, D.H., Patel, H.S., and Pandya, H.M., *Spectrochim. Acta, Part A*, 2010, vol. 75, no. 4, p. 1321.
12. Yadav, R.J., Vyas, K.M., and Jadeja, R.N., *J. Coord. Chem.*, 2010, vol. 63, no. 10, p. 1820.
13. *SMART and SAINT. Release 5.0. Area Detector Control and Integration Software,* Madison (WI, USA): Bruker AXS, Analytical X-ray Instruments, 1998.
14. Sheldrick, G.M., *SADABS. A Program for Exploiting the Redundancy of Area-Detector X-ray Data*, Göttingen (Germany): Univ. of Göttingen, 1999.
15. Sheldrick, G.M., *Acta Crystallogr., Sect. A: Found. Crystallogr.*, 2008, vol. 64, no. 1, p. 112.
16. Spek, A.L., *J. Appl. Crystallogr.*, 2003, vol. 36, no. 1, p. 7.
17. Becke, A.D., *J. Chem. Phys.*, 1993, vol. 98, no. 7, p. 5648.
18. Lee, C., Yang, W., and Parr, R.G., *Phys. Rev. B*, 1988, vol. 37, no. 2, p. 785.
19. Stratmann, R.E., Scuseria, G.E., and Frisch, M.J., *J. Chem. Phys.*, 1998, vol. 109, no. 19, p. 8218.
20. Frisch, M.J., Trucks, G.W., Schlegel, H.B., et al., *Gaussian'03. Revision D.01*, Wallingford (CT, USA): Gaussian, Inc., 2004.
21. Zhurko, G.A. and Zhurko, D.A., http://www.chemcraftprog.com
22. Rakitin, Yu.V., Larin, G.M., and Minin, V.V., *Interpretatsiya spektrov EPR koordinatsionnykh soedinenii* (Interpretation of EPR Spectra of Coordinatin Compounds), Moscow: Nauka, 1993.
23. Lebedev, Ya.S. and Muromtsev, V.I., *EPR i relaksatsiya stabilizirovannykh radikalov* (EPR and Relaxation of Stabilized Radicals), Moscow: Khimiya, 1972.
24. Wilson, R. and Kivelson, D.J., *Chem. Phys.*, 1966, vol. 44, no. 1, p. 154.
25. Popov, L.D., Levchenkov, S.I., Shcherbakov, I.N., et al., *Inorg. Chem. Commun.*, 2012, vol. 17, p. 1.
26. Shul'gin, V.F., Trush, Yu.V., Rusanov, E.B., et al., *Russ. J. Inorg. Chem.*, 2010, vol. 55, no. 5, p. 757.
27. Shul'gin, V.F., Trush, Yu.V., Konnik, O.V., et al., *Russ. J. Inorg. Chem.*, 2012, vol. 57, no. 2, p. 226.

Translated by D. Tolkachev